Complete Optimal Deployment Patterns for Full-Coverage and k-Connectivity ($k \leq 6$) Wireless Sensor Networks

Xiaole Bai† Dong Xuan† Ziqiu Yun‡ Ten H. Lai† Weijia Jia§
† Computer Science and Engineering, The Ohio State University, USA, {baixia,xuan,lai}@cse.ohio-state.edu
‡ Department of Mathematics, Suzhou University, CHINA, yunziqiu@public1.sz.js.cn
§ Department of Computer Science, City University of Hong Kong, CHINA, wjia@cs.cityu.edu.hk

ABSTRACT

In this paper, we propose deployment patterns to achieve full coverage and three-connectivity, and full coverage and five-connectivity under different ratios of sensor communication range (denoted by R_c) over sensing range (denoted by R_s) for wireless sensor networks (WSNs). We also discover that there exists a hexagon-based universally elemental pattern which can generate all known optimal patterns. The previously proposed Voronoi-based approach can not be applied to prove the optimality of the new patterns due to their special features. We propose a new deployment-polygon based methodology, and prove their optimality among regular patterns when $R_c/R_s \geq 1$. We conjecture that our patterns are globally optimal to achieve full coverage and three-connectivity, and full coverage and five-connectivity, under all ranges of R_c/R_s. With these new results, the set of optimal patterns to achieve full coverage and k-connectivity ($k \leq 6$) is complete, for the first time.

Categories and Subject Descriptors

C.2.1 [**Computer-Communication networks**]: Network Architecture and Design – *network topology*

General Terms

Theory

Keywords

Wireless sensor network topology, Optimal deployment pattern, Coverage, Connectivity

1. INTRODUCTION

Deployment is a fundamental issue in Wireless Sensor Networks (WSNs) that affects many facets of network operation, including routing, power management, security etc. Broadly, there are two categories of deployments in WSNs: random and deterministic deployments. Random deployments are typically the cases when the deployment area of the mission is physically inaccessible (e.g., volcanic, seismic zones etc.). Deterministic deployments on the other hand are more likely (and even preferable) in missions when the deployment area is physically accessible. The missions of deterministically deployed WSNs are increasingly becoming popular today. Instances include Line in the Sand [2] sensor network for target tracking, CitySense [9] network for urban monitoring, Soil Monitoring [8] sensor network etc., wherein sensors are hand-placed at selected spots prior to network operation. The success of such missions is tightly contingent on the optimality of deployment pattern. Fundamentally, knowledge of optimal deployment patterns will help avoid ad-hoc deployment (and likely inefficient patterns) by providing sound theoretical bounds. Optimal patterns also have benefits like cost savings (sensors still cost $100 apiece), minimizing message collisions, better network management etc. Furthermore, study of optimal patterns necessitates tremendous insights into network topology, which will provide a guideline for subsequent extensions of optimal patterns in non-ideal and more practical deployment scenarios.

However, exploring optimal patterns for WSNs is very hard, and has attracted researchers' attention for a long time. For years, works in sensor deployment are based on a result presented in 1939, which states that the regular triangular lattice pattern (triangle pattern in short) is asymptotically optimal in terms of the number of discs needed to achieve full coverage [7]. This result naturally provides six connectivity only when $R_c \geq \sqrt{3}R_s$. However, general values of R_c/R_s in practice can be anything positive. For example, while the reliable communication range of the Extreme Scale Mote platform is $30m$, the sensing range of the acoustics sensor for detecting an All Terrain Vehicle is $55m$ [1]. In this case, R_c/R_s is far less than $\sqrt{3}$. Progresses in exploring optimal patterns under different values of R_c/R_s have been made in recent years. In 2005, researchers proved that the strip-based deployment pattern is asymptotically near optimal when $R_c = R_s$ [6]. In 2006, the asymptotic optimality of strip-based deployment pattern to achieve one and two connectivity and full coverage was proved [3]. Furthermore, in a paper to be presented at Infocom 2008 [4], the asymptotically optimal pattern to achieve four connectivity and full coverage is explored. With the above progress made in this regard, two questions naturally arise:

- The work on exploring optimal patterns in WSNs is not complete yet. Is it possible to have a complete set of optimal patterns to achieve full coverage and k-connectivity? After all, there is no optimal pattern designed for 3-

MobiHoc'08, May 26–30, 2008, Hong Kong SAR, China.

connectivity and 5-connectivity. Different applications require different degrees of connectivity. Having a complete set of optimal patterns can meet the requirements of different applications.

- The previous exploration on optimal patterns has not yet been conducted in a systematic manner. Is there an elemental pattern that can generate all the patterns designed so far to achieve full coverage and k-connectivity? The existence of such a pattern can significantly and systematically help to explore other unknown patterns.

This paper aims to answer the above questions. Particularly, this paper makes the following contributions:

A complete set of deployment patterns: We propose new patterns for 3 and 5-connectivity. The pattern for 3-connectivity and 5-connectivity are both hexagon-based. With the newly proposed patterns, we have a complete set of optimal deployment patterns to achieve k-connectivity, for the first time. We prove the pattern optimality for $1 \leq R_c/R_s$, among regular deployment (patterns) defined in Section 2, and conjecture their global optimality for all the values of R_c/R_s [1]. Our numerical data show that 3-connectivity pattern can save up to 23% nodes, compared with the 4-connectivity pattern.

A universally elemental pattern: We discover that there exists a universally elemental pattern for full coverage and k-connectivity. The universally elemental pattern is hexagon-based and all known optimal patterns for different connectivity can be generated by repeating certain specific forms of it. In fact, we use this result in exploring the pattern for 5-connectivity.

A new proof methodology for optimality: The optimality of the patterns for 3 and 5-connectivity is hard to prove. Due to special features of these two patterns, the conditions necessary to apply the existing Voronoi-based methodology in [4][3] are not satisfied. We design a new deployment-polygon based approach for this purpose. This approach can be used to prove the optimality of the deployment patterns for both 3 and 5-connectivity, among regular patterns.

Paper Organization: We provide the system model in Section 2. In Section 3, we present our new proposed patterns for 3 and 5-connectivity and a whole picture of all optimal patterns for k-connectivity. Numerical results are also reported. In Section 4, we prove the optimality of the newly proposed patterns. In Section 5, we discuss some practical considerations. Section 6 concludes the paper.

2. SYSTEM MODEL

In this paper, we make several abstractions in order to obtain optimal deployment patterns in WSNs. Abstractions are inevitable in order to achieve enough generality when trying to lay down certain theoretical foundations. We will discuss practical considerations which are beyond the abstractions in Section 5. We also assume multiple sensors will

We use disc model for both sensing and communication. Each sensor is capable of detecting points only within distance R_s, and communicating only with others within distance R_c. Both R_s and R_c are invariant with respect to direction. This model has been widely adopted, e.g., in [3][4][6].

[1]We use the term *Global Optimality* to refer the asymptotical optimality among all possible deployments.

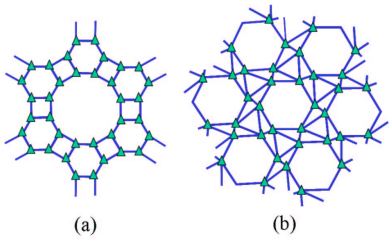

Figure 1: Deployment graphs for two possible regular deployments. Solid lines denote the communication links established. In (a), each vertex has degree of three. In (b) each vertex has degree of five.

We study the asymptotical optimality of deployment patterns. We consider a relatively large area compared with sensing and communication ranges. The boundary effect is not important and can be ignored.

We study the homogeneous wireless sensor networks where all the sensor nodes are identical in terms of sensing and communication capabilities. Since the sensors are homogeneous, it is natural to explore certain deployment where no sensors play special roles. For this purpose, we will introduce the concept of regular deployment. Before formally defining regular deployment, we first introduce some other definitions.

In our pattern exploring, we do not consider the possible patterns where multiple sensor nodes are deployed at the same location due to the fact these patterns may incur severe interference in reality. Then we have the following definitions.

DEFINITION 2.1. ***Communication Graph:*** *A communication graph, denoted by $G_c = (V_c, E_c)$, is a graph that is subject to the following conditions: 1) the elements of its vertices set V are sensors, and 2) the elements of its edge set E are straight line segments connecting all pairs of vertices with Euclid distance not larger than R_c.*

There is always a communication graph G_c corresponding to any given sensor deployment.

DEFINITION 2.2. ***Deployment Graph:*** *A deployment graph, denoted by $G = (V, E)$, is a planar subgraph of G_c with $V = V_c$ and $E \subseteq E_c$.*

There could be multiple deployment graphs corresponding to a given communication graph, and hence to a given deployment. A communication graph G_c naturally can be non-planar, i.e., the edges (straight line segments) may cross each other with the intersection points not at the vertices. Its deployment graph G can be constructed by removing some edges to make it planar.

DEFINITION 2.3. ***Direct Neighbor:*** *In a deployment graph $G = (V, E)$, if there is an edge between two vertices x and y, then x and y are direct neighbors of each other.*

DEFINITION 2.4. ***Angular Distance:*** *The angular distance between two vertices x and y as measured from a given vertex z is the degree of the angle $\angle xzy$.*

Denote the degree of a vertex x in G by k_x. It then has k_x direct neighbors. We denote its k_x neighbors by $n_1, n_2, \cdots,$

n_{k_x} in some order. We further denote the angular distance measured from x between n_1 and n_2 by α_{1_x}, between n_2 and n_3 by $\alpha_{2_x}, \cdots$, between n_{k_x-1} and n_{k_x} by α_{k_x-1} and between n_{k_x} and n_1 by α_{k_x}.

Now, we are ready to introduce the definition of regular deployment.

DEFINITION 2.5. ***Regular Deployment:*** *A sensor deployment is called regular if it has a deployment graph G where for any two vertices i and j in G, $k_i = k_j$ and $\alpha_{1_i} = \alpha_{1_j}, \alpha_{2_i} = \alpha_{2_j}, \cdots, \alpha_{k_i} = \alpha_{k_j}$ following the same order.*

Fig. 1 shows the deployment graphs of two possible regular deployment achieving 3 and 5-connectivity, respectively.

We wish to point out that, all known globally optimal deployment patterns including the triangular lattice pattern and the ones proposed in [3][4] are actually regular.

DEFINITION 2.6. ***γ-Optimal Pattern:*** *A regular deployment pattern is called γ-optimal if it needs the minimum number of sensors to achieve a given coverage and connectivity requirement, among all regular patterns.*

Studying γ-optimality of regular patterns is meaningful. Regular patterns have strong practical indications in homogeneous WSNs. Apparently, global optimality implies γ-optimality. In fact, we believe γ-optimality also implies global optimality. However, exploring (designing and proving) γ-optimal patterns is not trivial. The exploring space is still large, as demonstrated in the optimality proof of our proposed patterns in Section 4. There are a huge number of regular patterns for a given coverage and connectivity requirement, like ones illustrated in Fig. 1.

3. DEPLOYMENT PATTERNS

In this section, we first present a set of deployment patterns for 3-connectivity, and then present another set of patterns for 5-connectivity, both under different ranges of R_c/R_s. All these patterns are optimal or conjectured optimal. Finally, we present a complete picture of patterns to achieve k-connectivity, where $1 \leq k \leq 6$. We reveal that there exists a universally elemental pattern that all known optimal or conjectured-optimal patterns stem from.

3.1 Deployment Patterns for 3-Connectivity

In this subsection, we first present a general hexagon-based pattern for 3-connectivity. We then discuss its variations under different R_c/R_s.

In Fig. 2(b), we illustrate the hexagon-based pattern. It is a hexagon with all edges equal and opposite edges parallel. The parameters $\theta_1, \theta_2, \theta_3$ and d are the functions of R_c/R_s, which are expressed as follows:

$$\begin{cases} \theta_1 = \min\left(\pi, \max(\frac{2\pi}{3}, 4\arcsin\frac{R_c}{2R_s})\right), \\ \theta_2 = \max\left(\min(\frac{2\pi}{3}, 2\arccos\frac{R_c}{2R_s}), \right. \\ \qquad\qquad \left. \min(\frac{2\pi}{3}, 2\arcsin\frac{R_c}{2R_s})\right), \\ \theta_3 = 2\pi - \theta_1 - \theta_2, \\ d = \min(R_c, \sqrt{3}R_s). \end{cases} \quad (1)$$

For any value of R_c/R_s, these parameters guarantee that each point within the hexagon area can be covered by at least one of the sensors located at the vertices. Thus, when this hexagon-based pattern is repeated forming a complete tessellation, full coverage can be achieved. Furthermore, since d is always not greater than R_c, each sensor is guaranteed to have at least three communication links when this pattern is repeated, as shown in Fig. 2.

The hexagon-based pattern exhibits different forms (or patterns) under different values of R_c/R_s. Fig. 2(c) illustrates these variations:

- $R_c/R_s < 1$: The pattern is a regular hexagon with each edge length R_c, $\theta_1 = \theta_2 = \theta_3 = 2\pi/3$.
- $1 \leq R_c/R_s < \sqrt{2}$: The pattern is a flattened hexagon with edge length R_c. The top and bottom inner angles are $4\arcsin(R_c/2R_s)$ each, and the others are $2\arccos(R_c/2R_s)$ each.
- $R_c = \sqrt{2}R_s$: The pattern is a rectangular with side lengths $2R_c$ and R_c, respectively.
- $\sqrt{2} < R_c/R_s < \sqrt{3}$: The pattern becomes a parallelogram still with side lengths $2R_c$ and R_c. Its bigger inner angle is $2\arcsin(R_c/2R_s)$.
- $\sqrt{3} \leq R_c/R_s$: The pattern maintains a parallelogram but with side lengths $2\sqrt{3}R_s$ and $\sqrt{3}R_s$. The bigger inner angle for this parallelogram is $2\pi/3$.

The hexagon-based pattern is elemental. Its shape continuously changes in terms of $\theta_1, \theta_2, \theta_3$ and d, from a regular hexagon shape to a parallelogram shape, as the value of R_c/R_s increases. Full coverage and 3-connectivity run through all of these changes. In this paper, we are able to prove the patterns are γ-optimal when $1 \leq R_c/R_s$. The proof will be discussed in Section 4. We conjecture that the patterns are also globally optimal for all ranges of R_c/R_s.

3.2 Deployment Patterns for 5-Connectivity

In Fig. 3(b), we illustrate a pattern to achieve full coverage and 5-connectivity general for all values of R_c/R_s. It is a slim hexagon consisting of two equilateral triangles and one rhombus. The pattern can be expressed in term of $\theta_1, \theta_2, \theta_3$ and d as follows:

$$\begin{cases} \theta_1 = \frac{\pi}{3}, \\ \theta_2 = \frac{\pi}{3} + \min\left(\frac{2\pi}{3}, \max(\frac{\pi}{2}, 2\arcsin\frac{R_c}{2R_s})\right), \\ \theta_3 = 2\pi - \theta_1 - \theta_2, \\ d = \min(R_c, \sqrt{3}R_s). \end{cases} \quad (2)$$

These parameters ensure that each point within the hexagon area is covered by at least one of the sensors located at the hexagon vertices for any value of R_c/R_s. Notice the two sensors located at the top and bottom vertices have two communications links in the pattern respectively. As shown in Fig. 3(a) and (b), these two sensors will obtain another three communication links when the pattern is repeated. The other four sensors located at the vertices of the rhombus already have three communication links in the pattern respectively. As shown in Fig. 3, they will obtain another two links when the pattern is repeated. Hence, when this hexagon-based pattern is repeated forming a complete tessellation, full coverage and 5-connectivity both can be satisfied.

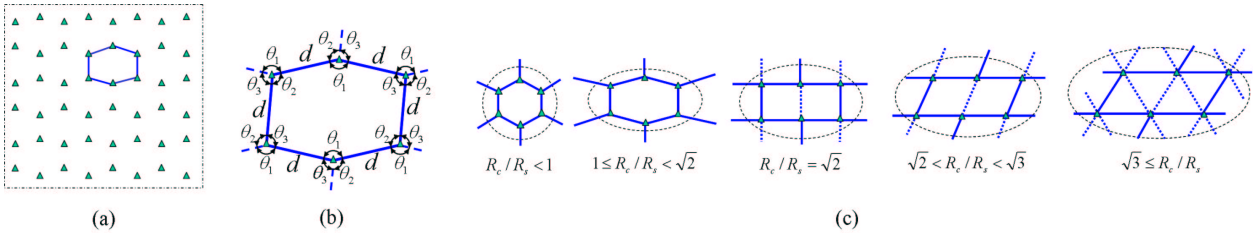

Figure 2: The hexagon-based pattern for 3-connectivity (a) and (b). In (c), R_s is fixed and R_c varies. The solid lines in (c) construct the patterns, denoting the established links. The dashed straight lines in (c) denote the links that can be established but not necessary.

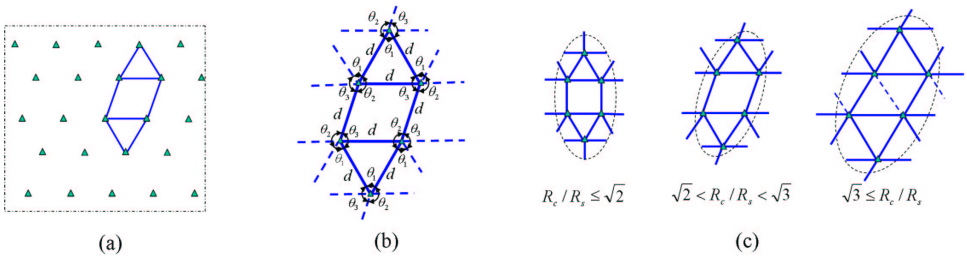

Figure 3: The hexagon-based pattern for 5-connectivity (a) and (b). In (c), R_s is fixed and R_c varies. The solid lines in (c) construct the patterns, denoting the established links. The dashed straight lines in (c) denote the links that can be established but not necessary.

The above general pattern in Fig. 3(b) exhibits different forms (or patterns) under different values of R_c/R_s. Fig. 3(c) illustrates these patterns:

- $R_c/R_s \le \sqrt{2}$: The rhombus becomes a square.
- $\sqrt{2} < R_c/R_s < \sqrt{3}$: The bigger inner angle of the rhombus is $2\arcsin(R_c/2R_s)$, which keeps increasing within $(\pi/2, 2\pi/3)$.
- $\sqrt{3} \le R_c/R_s$: The bigger inner angle of the rhombus is $2\pi/3$. The rhombus is constructed by putting together two equilateral triangles.

In this paper, we are able to prove the patterns are γ-optimal when $1 \le R_c/R_s$. We conjecture that the patterns are globally optimal for all ranges of R_c/R_s.

3.3 A Complete Set of Optimal Deployment Patterns

In this section, for the first time, we show in Fig. 4 the full extent of optimal patterns achieving full coverage and k-connectivity with $k = 1, 2, 3, 4, 5$ and 6, respectively. In Fig. 4, R_s is invariant. When R_c/R_s gets smaller (i.e. R_c decreases), sensors have to get closer to each other to satisfy the connectivity requirement, hence more sensors are needed to cover a given area.

We discover that there exists a universally elemental pattern. The universally elemental pattern is named such since all known optimal patterns for different connectivity can be generated by repeating certain specific forms of this pattern. This pattern is a hexagon with opposite sides are both equal and parallel that stratifies following two conditions: 1) given R_s, the inner area of this hexagon can be fully covered by the sensors deployed at the six vertices, and 2) given R_c, the tessellation constructed by repeating it can satisfy the desired connectivity.

The universally elemental pattern is illustrated in Fig. 5. Note that θ_3 can be decided by $\theta_3 = 2\pi - \theta_1 - \theta_2$. We denote a specific form of the universally elemental pattern for k connectivity by $H_k(\theta_1, \theta_2, d_1, d_2)$. By giving corresponding expressions for θ_1, θ_2, d_1 and d_2 in Fig. 4 right side, we show all known optimal deployments can be generated by repeating certain specific form of H_k.

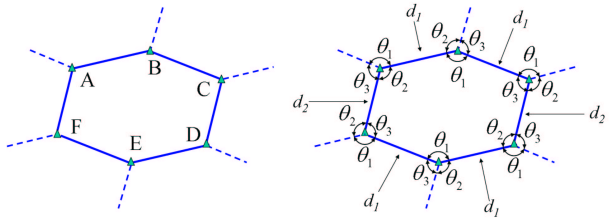

Figure 5: The universally elemental pattern.

For the strip based deployment pattern that is optimal to achieve full coverage and 2-connectivity (or 1-connectivity since its average degree is at least two asymptotically [3]), the specific form of the universally elemental pattern H_2 (or H_1) is shown in Fig. 6(a2). Fig. 6(a1) illustrates the distance between nodes AF and CD can be enlarged beyond R_c.

The specific form of H_4 in optimal deployment pattern to achieve full coverage and 4-connectivity is shown in Fig. 6(b2). Fig. 6(b1) and (b2) illustrate how this specific form of H_4 can be achieved from a general universally elemental pattern originally given.

For the optimal deployment pattern to achieve full coverage and 6 connectivity when $R_c \ge \sqrt{3}R_s$, the universally ele-

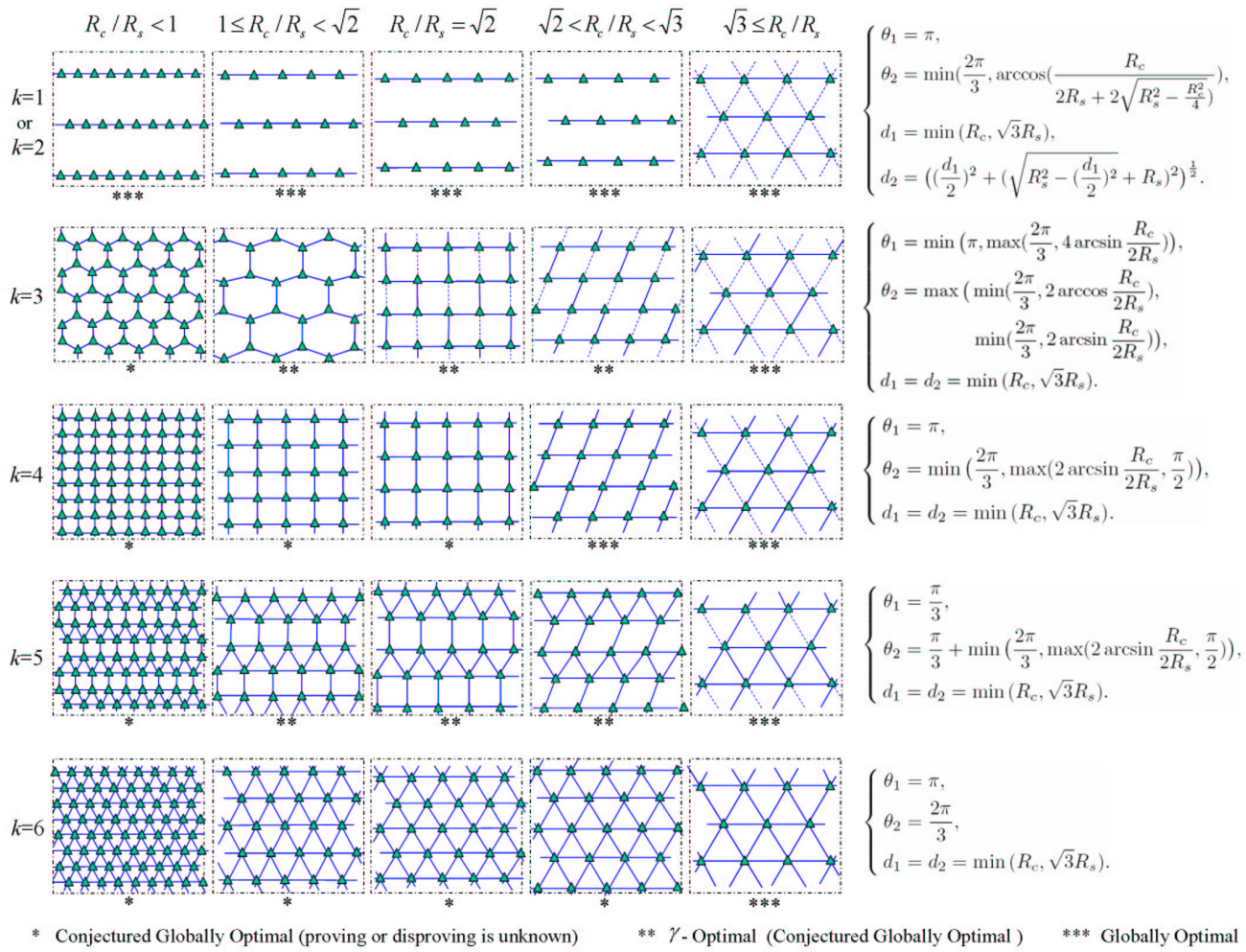

Figure 4: A complete set of optimal patterns achieving full coverage and k-connectivity with $k = 1, 2, 3, 4, 5$ and 6, respectively (where R_s is invariant and R_c varies). These patterns are specific forms of the universally elemental pattern defined by expressions of θ_1, θ_2,($\theta_3 = 2\pi - \theta_1 - \theta_2$), d_1 and d_2 on the right hand side of the above deployment patterns. Note that there are one and two vertical lines of nodes for global connectivity in 1 and 2-connectivity patterns, respectively. They are not shown for the sake of simplicity.

mental pattern H_6 takes a specific form shown in Fig. 6(c2). Fig. 6(c1) and (c2) illustrate how this specific form can be achieved by continuously adjusting sensor positions from a general universally elemental pattern originally given.

Remarks: The discovery of the universally elemental pattern significantly help to explore unknown optimal deployment patterns. In fact, following the lead of altering the shape of the universally elemental pattern to 4-connectivity and 6-connectivity patterns, i.e. from Fig. 6(b1) to Fig. 6(b2), and from Fig. 6(c1) to Fig. 6(c2), we are able to obtain the γ-optimal pattern for 5-connectivity shown in Fig. 3.

3.4 Numerical Results

In this subsection, we show the sensor number needed to achieve full coverage and $1 \sim 6$ connectivity respectively by optimal patterns shown in Fig. 4 for various R_c/R_s. Sensors each with sensing range $R_s = 30m$ are deployed over a $1,000m \times 1,000m$ deployment region. The communication range R_c varies from $20m$ to $60m$. From Fig. 7, we make following observations.

- Overall, the numbers of sensors required by individual patterns decrease as R_c/R_s increases. (Note that there is a slight difference in the numbers of nodes needed for 1-connectivity and 2-connectivity. The reason is that one extra vertical line of nodes are needed for 2-connectivity [3], compared with 1-connectivity.) Starting from $R_c/R_s = \sqrt{3}$, i.e. 1.732, all the patterns require the same amount of sensors, which reflects the fact that all the patterns merge with the triangular pattern at $R_c/R_s = 1.732$, as illustrated in Fig. 4. Similarly, the pattern for 3-connectivity requires the same number of nodes as that of the 4-connectivity starting from $R_c/R_s = \sqrt{2}$, i.e. 1.414, illustrating the fact that the former merges with the latter at the point of $R_c/R_s = 1.414$.

- The deployment pattern for 3-connectivity needs much less sensors than the one for 4-connectivity does, particularly, when R_c/R_s is small. For instance, when $R_c/R_s \le 1$, the sensor number needed by the former is only 77% of that of the latter. Both of them need more sen-

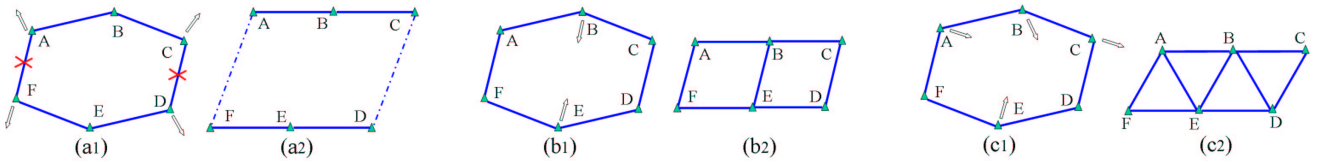

Figure 6: Specific forms of H_2(or H_1), H_4 and H_6 in the optimal deployment can be achieved by continuously adjusting sensor positions to enlarge the covered area, and to get communication links to meet required connectivity.

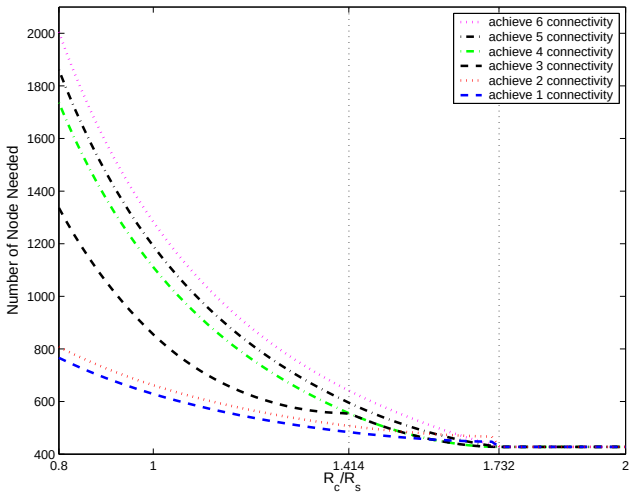

Figure 7: Number of nodes needed to achieve full coverage and $1 \sim 6$ connectivity respectively by optimal patterns. The region size is $1,000m \times 1,000m$. R_s is $30m$. R_c varies from $20m$ to $60m$.

sors than the stripe-based patterns for 1 and 2-connectivity. However, these patterns as well as those for 5, 6-connectivity can solve the long path problem existing in the the stripe-based patterns, as stated in [4].

- For all R_c/R_s, the sensor number needed for the pattern achieving 5-connectivity is roughly the average of the number needed for 4 and 6-connectivity. It is 93% of the number for 6-connectivity.

4. PATTERN OPTIMALITY

In this section, we first introduce some notations and definitons that will be needed in our optimality proof. We then explain why exploring optimality of patterns for 3 and 5-connectivity is hard, and show how to explore γ-optimality following our new methodology.

Recall Definition 2.2, and note that there are always deployment graphs corresponding to any given sensor deployment. If a deployment graph $G = (V, E)$ has k connectivity, we sometimes write $G_k = (V_k, E_k)$ to emphasize its connectivity. Note that every vertex $v \in V_k$ has degree at least k.

DEFINITION 4.1. ***Deployment Polygon:*** *A polygon (i.e., a simple cycle) in a deployment graph is called a deployment polygon.*

DEFINITION 4.2. ***Atomic Deployment Polygon:*** *An atomic deployment polygon, denoted by P^a, is a deployment polygon that contains no vertex or edge in its enclosed region.*

Note that an atomic deployment polygon does not "contain" any other deployment polygons.

4.1 Challenges

In general, proving the optimality of deployment patterns in WSNs is very hard. A Voronoi-based methodology was designed in [3][4], which can be used in the optimality proof of $1, 2$ and 4-connectivity patterns. However, due to the special features of 3 and 5-connectivity patterns, this methodology can not be applied.

The basic idea of this methodology is to take a sensor deployment as a tessellation of Voronoi polygons. The optimal deployment then implies a tessellation that covers the biggest area given the number of Voronoi polygons. The Voronoi-based methodology essentially considers coverage constraints explicitly through polygon area but the connectivity constraints can not be explicitly reflected. This methodology has its fundamental limitations. To apply this methodology, two conditions have to be satisfied: (1) the average edge number of Voronoi polygons generated by sensors has to be six. This condition stems from one boundary condition in Lemma 1 in [7], which suggests that in a tessellation of polygons, the average edge number of them will be not larger than six asymptotically. (2) The vertices of Voronoi polygons have to lie on the circumference of sensing discs. This condition comes from its limitation on reflecting the connectivity constraints implicitly.

Unfortunately, the patterns for 3 and 5-connectivity we presented in Section 3 violate the above conditions. As illustrated in Fig. 8(a), in patterns for 3-connectivity, the Voronoi polygon of each sensor owns three or four edges when $R_c/R_s \leq \sqrt{2}$, which clearly violates the first condition. As illustrated in Fig. 8(b), in patterns for 5-connectivity, the Voronoi polygon of each sensor has only five edges when $R_c/R_s \leq \sqrt{3}$. Also, the vertices of these Voronoi polygons do not lie on the circumference, which doesn't satisfy the second condition.

4.2 Optimality Proof

To explore the optimality for 3 and 5-connectivity patterns, we develop a new methodology based on the concept of atomic deployment polygon as defined before. Different from the Voronoi-based methodology, our new methodology essentially considers both coverage constraints and connectivity constraints explicitly. Coverage constraints are reflected by the area of atomic polygons while the connectivity constraints are embodied in the polygons edge length. This methodology then takes a sensor deployment as a collection of atomic deployment polygons, which form a tessellation over a region. Then an optimal deployment corresponds to a tessellation that covers the biggest area given the number of vertices constructing the polygons.

In the following, we will apply this new methodology in proving the γ-optimality of our proposed patterns. We will give the detailed proof for 3-connectivity patterns, and only

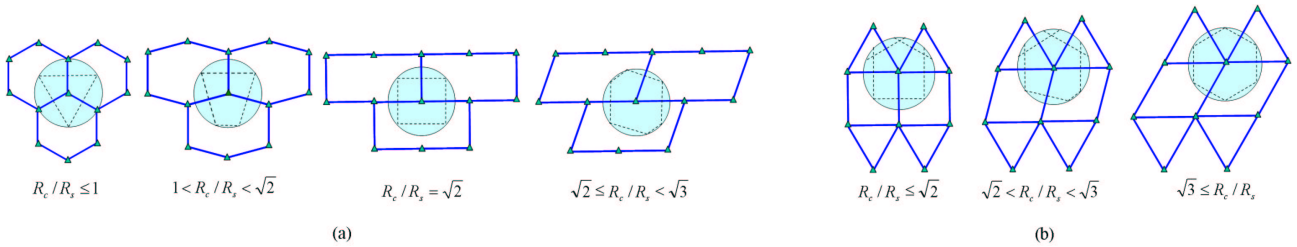

Figure 8: The shaded discs are the sensing discs. The dashed-lined polygons in (a) and (b) are the Voronoi polygons generated by one sensor in γ-optimal deployment of 3-connectivity and 5-connectivity, respectively.

sketch that for 5-connectivity patterns due to space limitations. The proof consists of three major steps:

In the first step, we prove that any regular deployment can be considered as a set of atomic deployment polygons covering the same area. The following Theorem 4.1 states this step. Note that in order not to interrupt the presentation of our main ideas, we defer some proofs to the Appendix.

THEOREM 4.1. *Let $\mathcal{A}$ denote a large square area. If $\mathcal{A}$ can be fully covered by a regular deployment of N sensors that achieves 3-connectivity, then $\mathcal{A}$ can be fully covered by a set of atomic deployment polygons constructed from N sensors such that the average edge number of them is not larger than six.*

Theorem 4.1 states a regular deployment that achieves full coverage and 3-connectivity can be considered as a set of P^as with certain characteristic. Lemma 4.1 is needed to prove this theorem.

LEMMA 4.1. *Given a deployment graph $G_k = (V_k, E_k)$ with $k > 2$, let μ_i denote the degree of $v_i \in V_k$ and ω the average edge number of atomic deployment polygons in G_k then*

$$\omega \le \frac{2\sum_{i=1}^{|V_k|} \mu_i}{\sum_{i=1}^{|V_k|} (\mu_i - 2)}. \quad (3)$$

Lemma 4.1 is important. It states the general relationship between deployment polygons and G_k for any $k > 2$.

Now we sketch the proof for Theorem 4.1.

PROOF. Any G_3 can be considered as a union of a set of non-overlapping deployment polygons. Also, each deployment polygon in G_3 can be further considered as the union of a set of P^as.

Fig. 9(a) shows the case where a deployment polygon is not atomic but contains no other polygons. It can be proved by contradiction that in such a case there must be at least one vertex that has degree of one or zero. It does not exit in G_3 since it violates the connectivity requirement.

Any deployment polygon in G_3 that is not atomic can be decomposed into a set of P^as. Fig. 9(b) shows an example. Since there must be a set of deployment polygons covering $\mathcal{A}$, there must also be a set of P^as covering $\mathcal{A}$.

In a regular deployment that achieves 3-connectivity, each vertex has degree of three. From Lemma 4.1, the average number of these P^as will not greater than six when $\mu_i = 3$ for each v_i. □

In the second step, we prove that the pattern we proposed in Fig. 2 is optimal for $1 \le R_c/R_s$ among the sets wherein each atomic deployment polygon is a hexagon. Let the area

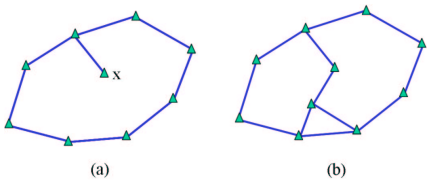

Figure 9: (a) In a deployment polygon that is not atomic but contains no other polygons, vertex x has degree of one. (b) An example: a big deployment polygon can be decomposed into three atomic ones.

of the hexagon pattern (and its variations) proposed in Fig. 2 for 3-connectivity be denoted by S_6 That is, S_6 is the area of the hexagons decided by parameters in (1). We then have following Theorem 4.2.

THEOREM 4.2. *When $1 \le R_c/R_s$, the maximum area of a hexagon, where each edge is at most R_c and each point within the hexagon can be covered by at least one of the sensors located at the vertices, is S_6.*

PROOF. We sketch the proof below. Formula derivations are omitted due to space limitations.

We first show that, given a n-sided polygon with edges $e_1 e_2 \cdots e_n$ where the length of one edge e_1 is fixed and the total length of other edges is also fixed, its area achieves the maximum when its edges $e_2, e_3, \cdots, e_n$ are of the same length. Assume that the polygon already achieves its maximum area while there are still at least two edges not equal. We can then find a pair of neighboring edges with different lengths. Denote them by e_i and e_{i+1}. Suppose the length of e_i is less than that of e_{i+1}, and their joint vertex is x. We can always further increase the area of the polygon by moving x such that the length of e_i is increased to the length of e_{i+1}.

We then consider the hexagons with equal edge length R_c. We divide the hexagon with vertices $abcdef$ into two quadrilaterals by connecting a diagonal be. When the length of the diagonal is fixed, the area of the quadrilaterals achieves the maximum when it is an isosceles trapezoid. The area of this isosceles trapezoid changes as the length of the diagonal alters. Since every point within the hexagon has been covered, every point within the isosceles trapezoid should also be covered by at least one sensor at its vertices.

When $1 \le R_c/R_s \le \sqrt{2}$, the area of this isosceles trapezoid takes the maximum value as the length of the diagonal be is $2R_s \cos(\pi - 3\arccos(R_c/2R_s))$. Furthermore, the maximum area is a increasing function of R_c. Fig. 10 shows the isosceles trapezoid that can be covered by sensors at its vertices. When

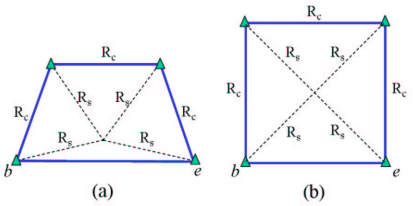

Figure 10: (a) The isosceles trapezoid when $1 < R_c/R_s < \sqrt{2}$. (b) The isosceles trapezoid when $R_c/R_s = \sqrt{2}$.

$R_c/R_s = \sqrt{2}$, the length of the diagonal be becomes R_c and the isosceles trapezoid becomes a square.

When $\sqrt{2} < R_c/R_s$, the maximum area is achieved when the hexagon is the union of two rhombuses. The proof follows the same way as that for Theorem 5.1 in [3]. □

In the third step, we prove the pattern we proposed in Fig. 2 actually covers the biggest area among all the polygon sets that are also capable of constructing regular deployment satisfying the same requirement, i.e., to achieve full coverage and 3-connectivity. The following Theorem 4.3 states this.

THEOREM 4.3. *When $1 \leq R_c/R_s$, among all atomic deployment polygon sets that are of N sensors and can construct a regular deployment satisfying full coverage and 3-connectivity, the set whose elements all have area S_6 covers the biggest area.*

The proof for Theorem 4.3 is hard, for which the following Lemma 4.2 is needed. Lemma 4.2 states the covered area of a specific type of sensor deployment is bounded. We sketch their proofs in the Appendix.

LEMMA 4.2. *If G_3 is constructed by a set of different types of P^as, among which those with the largest number of edges are regular polygons, then the average area of the P^as in this set will not be larger than a regular hexagon with edge length R_s.*

The following theorem concludes the γ-optimality proof for 3-connectivity patterns we proposed in Fig. 2.

THEOREM 4.4. *When $1 \leq R_c/R_s$, the patterns proposed in Fig. 2 are γ-optimal to achieve full coverage and 3-connectivity.*

Theorem 4.4 follows Theorem 4.3 naturally. The area covered by any sets of P^as will not be larger than that covered by a set of P^as each with area S_6. Hence, the deployment pattern constructed by this set of P^as each with area S_6 is the optimal among all deployment patterns.

Following the same three steps above, we can prove the γ-optimality for 5-connectivity patterns when $1 \leq R_c/R_s$ similarly. We only list four important related theorems below. Due to space limitation, all their proofs are omitted in this paper.

In the first step, we have Theorem 4.5:

THEOREM 4.5. *Let $\mathcal{A}$ denote a large square area. If $\mathcal{A}$ can be fully covered by a regular deployment of N sensors achieving 5-connectivity, then $\mathcal{A}$ can be fully covered by a set of atomic deployment polygons constructed from N sensors such that the average edge number of them is not larger than $10/3$.*

In the second step, we have Theorem 4.6. Let the area of hexagon pattern (and its variations) proposed in Fig. 3 for 5-connectivity be denoted by S_6'.

THEOREM 4.6. *When $1 \leq R_c/R_s$, the maximum area of the hexagon that contains two triangles and a rhombus, where each edge is less than R_c and each point within the hexagon can be covered by at least one of the sensors located at the vertices, is S_6'.*

In the third step, we prove the pattern we proposed in Fig. 3 actually covers the biggest area among all the polygon sets that are also capable of constructing some regular deployment achieving 5-connectivity.

THEOREM 4.7. *When $1 \leq R_c/R_s$, among all atomic deployment polygon sets that are of N sensors and can construct a regular deployment satisfying full coverage and 5-connectivity, the set only consisting of triangles and rhombuses where the number of triangle is two times of the number of rhombus and total area of any two triangles and one rhombuses is S_6' covers the biggest area.*

Remarks: The limitation for our methodology in pr-oving the global optimality mainly steps from the third step of the above proof. The regularities from regular deployment patterns have to be exploited to narrow the searching space in the optimality proof at that step. However, as shown in the Appendix, there are still a lot of cases needed to be considered in the proof of Theorem 4.3.

5. PRACTICAL CONSIDERATIONS

We discuss some practical considerations which are beyond the abstractions made in Section 2 below.

On Non-disc sensing and communications models: In practice, the disc models do not always coincide empirical observations. It is suggested the quality of sensing could gradually attenuate with increasing distances. Cao *et al.* in [5] suggest the sensing range of passive infrared (PIR) sensor roughly follows two dimensional Gaussian distribution. Studies have also suggested that wireless communication links could be irregular and being non-disc. In [10], Moscibroda *et al.* propose the SINR model which implies that a receiver may not be able to receive signals correctly even when it is close to the sender because of interference and noise effects. The disc model can be considered a clean abstraction ignoring any uncertain physical disruptions. It also can be considered a conservative measure. For instance, we can set a conservative threshold to get R_s in the probabilistic sensing cases, and get a conservative R_c by taking the lower bound in some non-disc communication cases. Exploring the optimal deployment patterns for the sensors with specific characteristics, is part of our future research.

On geographical constraints in sensor deployment: In practice, the sensor deployment field is bounded. Optimality is affected by the boundary. However, if different boundary shapes are considered, there can be numerous specific scenarios. There is another type of geographical constraints. In some fields, sensors cannot be placed in practice at desired spots (due to rocks, ponds etc), although theoretically those spots are optimal. With the above constraints, optimal deployment cannot be achieved. However, the optimal deployment patterns can act as references to guide real-world deployment to avoid ad-hoc deployments.

On heterogeneity of sensor nodes: Sensor nodes may not be homogenous. It may also happen that there are certain gateways (a multi-tiered sensor network structure), where the

gateway routes data between sensors and the base station. In such cases, optimality must be provided to both sensors and gateways. Our proposed optimal patterns are still valuable. A simple example is as follows. Let us consider the sensor to gateway communication range as R_s, and the gateway to gateway communication range as R_c. Ensuring that the full network is full-covered (with coverage range R_s) with k-connectivity (with communication range R_c) means that each sensor in the network can communicate with at-least one gateway, while each gateway has k-connectivity to other gateways. There can be other enormous specific scenarios of heterogeneity in sensor nodes. Exploring optimal patterns for all these scenarios is very hard, if not impossible.

6. CONCLUSION

In this paper, we proposed optimal deployment patterns to achieve full coverage and 3-connectivity; and full coverage and 5-connectivity for WSNs. With these results, the set of patterns to achieve full coverage and k-connectivity ($k \leq 6$) is complete. We also demonstrated that there exists a hexagon-based universally elemental pattern which can be used to generate all other patterns. To prove the optimality of newly designed patterns, we proposed a new deployment-polygon based methodology, which is different from the previously proposed Voronoi-based one.

We were able to prove the γ-optimality for the new proposed patterns, and conjectured their global optimality. The proof of the global optimality for the newly proposed patterns, as well as for the ones in Fig. 4 is part of our future research work. As stated before, extending our proposed patterns under non-disc sensing and communication models is also one of our future research directions.

7. ACKNOWLEDGEMENT

This work was supported in part by the US National Science Foundation (NSF) CAREER Award CCF−0546 668, the Army Research Office (ARO) under grant No. AMSRD−ACC−R 50521−CI, National Science Foundation of China (NSFC) grant No. 10571151, SAR Hong Kong RGC Competitive Earmarked Research Grant (CE RG) No. 9041129 (CityU 113906), CityU Strategic Research Grant (SRG) No. 7002102 and 7002214. Any opinions, findings, conclusions, and recommendations in this paper are those of the authors and do not necessarily reflect the views of the funding agencies.

8. REFERENCES

[1] A. Arora, et. al. ExScal: Elements of an Extreme Scale Wireless Sensor Network. In *11th IEEE International Conference on Real-Time Computing Systems and Applications,* 2005.

[2] A. Arora, et. al. A Line in the Sand: A Wireless Sensor Network for Target Detection Classification and Tracking. *Computer Networks,* 2004.

[3] X. Bai, S. Kumar, D. Xuan, Z. Yun and T. H. Lai. Deploying Wireless Sensors to Achieve Both Coverage and Connectivity, *ACM Mobihoc,* 2006.

[4] X. Bai, Z. Yun, D. Xuan, T. H. Lai and W. Jia. Deploying Four-Connectivity And Full-Coverage Wireless Sensor Networks. *IEEE INFOCOM,* 2008.

[5] Q. Cao, T. Yan, J. A. Stankovic, and T. F. Abdelzaher. Analysis of Target Detection Performance for Wireless Sensor Networks. *International Conference on Distributed Computing in Sensor Networks,* 2005.

[6] R. Iyengar, K. Kar and S. Banerjee. Low-coordination Topologies for Redundancy in Sensor Networks. *ACM Mobihoc,* 2005.

[7] R. Kershner. The Number of Circles Covering a Set. *American Journal of Mathematics,* 1939.

[8] research.cens.ucla.edu/projects/2006/ Contaminant/ Multiscale Soil/default.htm

[9] R. Narayana Murty, et. al. www.eecs.harvard.edu/ ∼mdw/papers/ citysense-techrept07.pdf.

[10] T. Moscibroda, R. Wattenhofer and A. Zollinger, Topology Control Meets SINR: The Scheduling Complexity of Arbitrary Topologies, *ACM Mobihoc,* 2006.

Appendix

Some lemmas and theorems were not proved in Section 4.2. We sketch their proofs here. The detailed derivations are omitted due to space limitations. For more details, please refer to our technical report.

Proof for Lemma 4.1.

Any planar deployment graph G_k with $k > 2$ can be considered as a non-overlapped tiling of a set of deployment polygons. Let the number of deployment polygons in G_k be denoted by N_P. Then from Euler relationship, we have

$$|V_k| - |E_k| + N_P = 1.$$

Since each edge has two vertices, $\sum_{i=1}^{|V_k|} \mu_i = 2|E_k|$. Replacing it into Euler relationship, we obtain

$$\sum_{i=1}^{|V_k|}(\mu_i - 2) + 2 = 2N_p.$$

Notice $\mu_i - 2 > 0$ since $k > 2$. We then have

$$\omega = \frac{\sum_{i=1}^{|V_k|} \mu_i}{N_p} = \frac{2\sum_{i=1}^{|V_k|} \mu_i}{\sum_{i=1}^{|V_k|}(\mu_i - 2) + 2} \leq \frac{2\sum_{i=1}^{|V_k|} \mu_i}{\sum_{i=1}^{|V_k|}(\mu_i - 2)},$$

where the last equality holds asymptotically.

Proof sketch for Lemma 4.2.

Consider the polygons with the largest number of edges in a set of P^as. Denote their edge number by m and edge length by l. If they are regular polygons, the distance between their vertices to their centers must be less than R_s due to the requirement to achieve full coverage. Then we transform them into new regular polygons with m edges whose vertices all lie on the circumference of the disc with radii R_s. Denote the edge length for these new regular polygons are l'. Note this transformation does not change the edge number, and the area of each polygon will not be decreased during transformation since $l' \geq l$.

We then consider the polygons with number of edges smaller than m in the set. Pick a polygon among them. Let its edge number be denoted by n, $n < m$. Its edge length is also l, since we only need to consider the P^a sets where every edge has the same length from the proof for Theorem 4.2. We also transform it into a new regular polygon with n edges whose vertices all lie on the circumference of the disc with radii R_s. Denote the edge length for this new regular polygons are l''. Since $n < m$, we have $l'' > l'$. So $l'' > l$. Hence, this transfor-

mation does not change the edge number, and the area of the polygon will not be decreased during transformation.

Now we have a new set of P^as wherein each polygon is a regular one and its vertices all lie on the circumference of the disc with radii R_s. From Lemma 1 and Lemma 2 in [7], the average area of the polygons in this set is less than the area of a regular hexagon inscribed in a disc with radii R_s.

Proof sketch for Theorem 4.3.

Let $\mathcal{S}_{S_6}$ denote a set whose elements are P^as each with area S_6. This set can construct a regular deployment satisfying full coverage and 3-connectivity. We are now considering all other possible sets that can can also construct such a deployment.

Case 1. If in a set the P^a with the maximum number of edges is a regular polygon, then from Lemma 4.2 this kind of set will not cover more area than $\mathcal{S}_{S_6}$ does.

Case 2. If a set only contains one kind of P^as, then from Theorem 4.2, this kind of set will also not cover more area than $\mathcal{S}_{S_6}$ does.

Case 3. We are now considering the case when the set contains more than one types of P^as and the P^a with the maximum number of edges is not a regular one. There are only three different angles in each set. And the sum of these three angles is 2π. Since the P^a with the maximum number of edges is not regular, the P^as in the set can not be all the regular polygons. There are following cases then.

Case 3.1. All P^as in the set are not regular.

Case 3.1.1. There are two types of P^as with two different inner angles in each P^a.

One of two inner angles is common between two types of P^as. From Theorem 4.1, there is at least one type of P^a with side number less than six. Note that, if a pentagon with all edges equal and at most two different inner angles, it must be a regular pentagon. Also note a triangle with all edges equal is a equilateral (regular) triangle. Hence, the P^a with the less number of edges must be a rhombus. In a rhombus, the sum of two different inner angles is π. Since the three angles at a vertex should be with sum of 2π, the third angle must be π. Thus, the P^a with edge number larger than six will have this angle of π, which actually will not be an inner angle. So the two types of the inner angles in it will be the two types of inner angle in the rhombus. Hence, the P^a with edge number larger than six is also a rhombus with each side length two times of R_c and inner angles the same as those in the small rhombus. When satisfying the full coverage, the covered area of the set containing these two P^as is less than $\mathcal{S}_{S_6}$ does.

Case 3.1.2. There are two types of P^as. One type of P^a has two different inner angles, while the other type has three.

Two of three types of inner angle in the latter type are the same as those in the former type. The equilateral (regular) triangle can not be such P^as since there is only one type of inner angle of $\pi/3$. There are at most two different types of inner angles in a rhombus. And the sum of them is π. This will be the same case as Case 3.1.1. Hence, in this case, the only subcase we should consider is that when the P^as with side number less than six are pentagons. However, given a pentagon with all edges equal, it will be a regular pentagon or has at least three different types of inner angles. So the type of of P^a that has three different types of inner angles must be pentagon. Note that the sum of these three different inner angles is 2π and the sum of all inner angles in a pentagon is 3π. It implies that one inner angle in this pentagon must be π, which is impossible.

Case 3.2. Only one type of P^a in the set is regular. In this case, the edge number of each regular P^a is less than six. Otherwise, the P^a with the maximum edge number must be a regular one, which is the Case 1. And the edge number of each irregular P^a must be larger than six. We have three subcases to study in this case. Case 3.2.1: The set contains the regular pentagons and another type of irregular P^a. Case 3.2.2: The set contains the squares and another type of irregular P^a. Case 3.2.3: The set contains the equilateral triangles and another type of irregular P^a.

The last case to study is Case 3.3 where in the polygon set, there are two types of P^as that are regular, and the P^a with the maximum edge number is not regular.

The proofs for the above cases are tremendous. We omit them due to space limitations.

Proof sketch for Theorem 4.5.

The proof is similar to that for Theorem 4.1 with $\mu_i = 5$.

Proof sketch for Theorem 4.6.

The proof is similar to that for Theorem 5.1 in [3].

Proof sketch for Theorem 4.7.

We first prove the following lemma.

LEMMA 8.1. *In a non-regular polygon with edge number larger than four and all edges equal, we can pick two different inner angles with sum larger than π.*

PROOF. Let n denote the side number of the polygon with all edges equal. When $n > 4$, it is impossible for this polygon to have $n-1$ inner angles that are equal and the left one take different angle. We can assume that n inner angles satisfy $a_1 \leq a_2 \leq a_3 \cdots \leq a_n$. Let $a = (a_1+a_2)/2$ and $b = (a_3+\cdots+a_n)/(n-2)$. Then $a_2 > a$ and $a_n > b$. Since $2a + (n-2)b = (n-2)\pi$, we have $b = \pi - 2a/(n-2) > \pi - a$. Hence, $a_2 + a_n \geq a + b > \pi$. □

Now we sketch the proof for Theorem. From Lemma 4.1, we have the average edge number for a set of P^es constructing a deployment pattern where there are 5 edges at each vertex will not be larger than $10/3$. Then in such a set of P^e, there must be equilateral triangles. Otherwise, the average edge number must be at least four.

Now consider the case when there are pentagon P^es. If the pentagon are regular, there must be other types of polygon in the set since it is impossible to choose five angles among those equal to 108° or $\pi/3$ to construct 2π. Notice in a rhombus the sum of the different inner angles is π. A pair of such angles with sum equal to π still can not construct 2π together with three angles among those equal to 108° or $\pi/3$. So the other type of polygon can not be rhombus. Hence, the pentagon can not be the regular pentagon. Now consider the case when the pentagon are not regular. Then there must be three different types of inner angle at a pentagon. The sum of three inner angles from these three types respectively will larger than 270°. They are three of the five angles at each vertex. But the average of the left two angles will be less than $\pi/3$, which is impossible. Hence, there will not be pentagon P^es.

It can be shown similarly, supported by Lemma 8.1, it is either impossible to have other P^es with edge number larger than five to construct a regular 5-connectivity network, or it is possible to construct the deployment graph that meets the coverage and connectivity requirement, but the average area of each atomic polygon is less than $S_6'/3$.